

Similar zone-center gaps in the low-energy spin-wave spectra of $\text{Na}_{1-\delta}\text{FeAs}$ and BaFe_2As_2

J. T. Park,¹ G. Friemel,¹ T. Loew,¹ V. Hinkov,^{1,2} Yuan Li,^{1,3} B. H. Min,⁴ D. L. Sun,¹ A. Ivanov,⁵ A. Piovano,⁵ C. T. Lin,¹ B. Keimer,¹ Y. S. Kwon,^{4,*} and D. S. Inosov^{1,†}

¹Max-Planck-Institut für Festkörperforschung, Heisenbergstraße 1, 70569 Stuttgart, Germany

²Quantum Matter Institute, University of British Columbia, Vancouver, BC, Canada V6T 1Z1

³International Center for Quantum Materials, School of Physics, Peking University, Beijing 100871, China

⁴Department of Emerging Materials Science, DGIST, Daegu 711-873, Republic of Korea

⁵Institut Laue-Langevin, 6 rue Jules Horowitz, 38042 Grenoble Cedex 9, France

(Received 31 March 2012; revised manuscript received 13 May 2012; published 27 July 2012)

We report results of inelastic-neutron-scattering measurements of low-energy spin-wave excitations in two structurally distinct families of iron-pnictide parent compounds: $\text{Na}_{1-\delta}\text{FeAs}$ and BaFe_2As_2 . Despite their very different values of the ordered magnetic moment and Néel temperatures, T_N , in the antiferromagnetic state both compounds exhibit similar spin gaps of the order of 10 meV at the magnetic Brillouin-zone center. The gap opens sharply below T_N , with no signatures of a precursor gap at temperatures between the orthorhombic and magnetic phase transitions in $\text{Na}_{1-\delta}\text{FeAs}$. We also find a relatively weak dispersion of the spin-wave gap in BaFe_2As_2 along the out-of-plane momentum component, q_z . At the magnetic zone boundary ($q_z = 0$), spin excitations in the ordered state persist down to ~ 20 meV, which implies a much smaller value of the effective out-of-plane exchange interaction, J_c , as compared to previous estimates based on fitting the high-energy spin-wave dispersion to a Heisenberg-type model.

DOI: [10.1103/PhysRevB.86.024437](https://doi.org/10.1103/PhysRevB.86.024437)

PACS number(s): 75.30.Ds, 74.70.Xa, 78.70.Nx

I. INTRODUCTION

The discovery of unconventional superconductivity in iron-pnictide compounds¹ with critical temperatures, T_c , as high as 56 K has fostered a tremendous interest in these materials in recent years.² There are several structurally distinct families of iron-based superconductors with similar phase diagrams,² governed by an interplay of antiferromagnetism, persistent in pure compounds under ambient pressure, and superconductivity that can be induced by pressure or chemical doping.³ Although the highest values of T_c are usually found in doped compounds with a nonstoichiometric composition, our physical understanding of these systems undoubtedly depends on the detailed knowledge of magnetic properties in the respective parent compounds, which are also easier to treat theoretically due to their simple crystal structure with no substitutional disorder.

Among the variety of such stoichiometric materials serving as parent phases for numerous iron-based superconductors, only a few have so far received proper experimental treatment, especially by inelastic neutron scattering (INS), due to miscellaneous reasons related to the availability of sizable single crystals or their chemical stability. For instance, to the best of our knowledge, direct measurements of spin-wave excitations in the antiferromagnetic (AFM) state of iron pnictides have so far remained limited to a few members of the so-called “122” family with the ThCr_2Si_2 -type structure, whose single crystals are typically stable in air and are readily available in the large sizes necessary for INS experiments. In particular, high-energy spin-wave modes have been mapped out in CaFe_2As_2 ^{4,5} and BaFe_2As_2 ⁶ using time-of-flight (TOF) neutron spectroscopy, which enabled estimations of the effective magnetic exchange interactions in the framework of a localized Heisenberg-type $J_{1a}-J_{1b}-J_2-J_c$ model. These results are complemented by INS measurements at lower energies, performed on polycrystalline BaFe_2As_2 ⁷ and on single crystals of SrFe_2As_2 ,⁸ CaFe_2As_2 ,^{9,10}

and BaFe_2As_2 .¹¹ All of these measurements have unequivocally demonstrated the existence of a large anisotropy gap in the spin-wave dispersion at the magnetic Brillouin-zone center, which varies from 6.5–7.0 meV in SrFe_2As_2 and CaFe_2As_2 ^{8–10} to almost 10 meV in BaFe_2As_2 .^{7,11} A more recent polarized INS experiment has revealed two distinct components of this gap in BaFe_2As_2 , characterized by the out-of-plane and in-plane polarizations,¹² with the onsets at 10 meV and 16 meV, respectively.

At present, first-principles calculations are faced with apparent difficulties in reproducing these energy scales in the spin-wave spectra even on a qualitative level.^{12,13} Moreover, the identical crystal structure of all measured compounds, distinct from the structures of other families, precludes generalizations to all iron pnictides, making it difficult to relate the measured gaps to such microscopic structural and magnetic properties of the material as the ordered magnetic moment, exchange interactions, or crystallographic parameters. Therefore, in the present study we have performed INS measurements of the low-energy spin-wave spectrum in $\text{Na}_{0.9}\text{FeAs}$ ¹⁴ with the “111”-type structure, which we compare to that of BaFe_2As_2 .

II. SAMPLE CHARACTERIZATION

A single crystal of $\text{Na}_{1-\delta}\text{FeAs}$ with a small Na deficiency, $\delta \approx 0.1$, as estimated by energy-dispersive x-ray analysis, and a mass of ~ 0.5 g was grown by the vertical Bridgman method.¹⁵ Pure $\text{FeAs}_{1.17}$ precursors were first synthesized from the reaction of high-purity Fe (powder, 99.999%) and As (chips, 99.999%) in sealed quartz containers at 1050 °C. A $\text{Na}_{0.9}\text{FeAs}$ single crystal was then grown from a mixture of Na and precursor $\text{FeAs}_{1.17}$ with a molar ratio of 2:1 in a sealed molybdenum crucible. Higher molar concentrations of Na and As were necessary because of their high vapor pressures.

During growth, the center of the furnace was heated to 1450 °C. Because of the extreme chemical sensitivity of $\text{Na}_{1-\delta}\text{FeAs}$ to oxygen and air moisture,¹⁶ meticulous care had to be taken to exclude any contact with air while handling the crystal over the entire process of sample preparation and measurements. Prior to the INS experiment, the crystal had been sealed inside an aluminum can in helium atmosphere and oriented using a 4-circle neutron diffractometer *Morpheus* of the Paul Scherrer Institute (PSI), Switzerland. These preliminary measurements indicated that the sample consists predominantly of one single-crystalline grain with a mosaicity $<0.5^\circ$. Our second sample was a mosaic of BaFe_2As_2 single crystals with a total mass of ~ 0.9 g, grown by the self-flux method as described elsewhere,¹⁷ coigned on a silicon wafer using x-ray Laue diffraction to a mosaicity $\lesssim 1.0^\circ$.

A remarkable property of the $\text{Na}_{1-\delta}\text{FeAs}$ compounds is the large splitting in temperature between the magnetic and structural phase transitions, which is present even in the parent phase,^{18–21} whereas in the “122” family of iron pnictides the two transition temperatures usually merge together upon the reduction of doping.^{22–25} This makes it possible to study the narrow temperature window between the two transitions, which is typically associated with a so-called “electronic liquid crystal” (or “spin nematic”) phase with a spontaneously broken rotational symmetry of the electronic eigenstates. In our $\text{Na}_{0.9}\text{FeAs}$ sample, the AFM and orthorhombic phase transitions appear as anomalies in the temperature derivative of the magnetization [Fig. 1(a)] and in the order-parameter-like dependencies of the magnetic and nuclear Bragg peak intensities [Figs. 1(b) and 1(c)], respectively. From these measurements, the corresponding transition temperatures, $T_N = 45$ K and $T_s = 57$ K, could be determined, which are in agreement with literature values for samples of similar composition.^{18–21} Although the orthorhombic distortion is too weak to be directly resolved as the splitting of Bragg reflections in our experiment, the abrupt change in the (200) nuclear Bragg intensity at T_s , seen in Fig. 1(c), is explained by the extinction release associated with a minor change in the sample’s mosaicity across the orthorhombic transition, and has been previously used by several authors as a convenient and highly sensitive probe of the weak structural distortion.^{24–26} In addition, our $\text{Na}_{0.9}\text{FeAs}$ sample exhibits a weak superconducting (SC) transition at $T_{c, \text{onset}} \approx 8$ K, but the volume fraction of the SC phase is below 10%, according to magnetization measurements [Fig. 1(a), inset], and can be therefore neglected for the purpose of the present study. In BaFe_2As_2 , both neutron diffraction and magnetization measurements (not shown) have revealed the AFM ordering below $T_N = 137$ K, in agreement with previous reports.²²

III. INELASTIC NEUTRON SCATTERING

A. Zone-center gap

Unprocessed INS data shown in Fig. 2 illustrate several representative momentum scans along the $|\mathbf{Q}| = \text{const}$ trajectories in the $(H0L)$ plane, measured on both samples above and below T_N in the spin-gap region. Here and henceforth, we are using the unfolded reciprocal-space notation of the Fe sublattice because of its simplicity and the natural

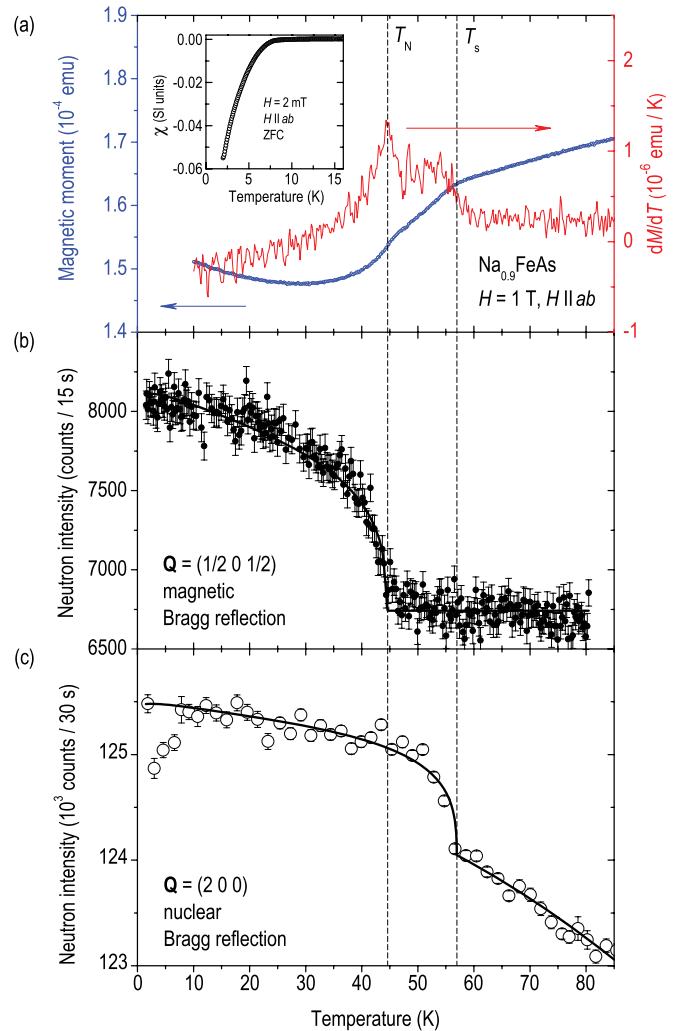


FIG. 1. (Color online) Determination of the structural and AFM transition temperatures in $\text{Na}_{0.9}\text{FeAs}$ from (a) magnetization measurements, (b) magnetic Bragg intensity, and (c) nuclear Bragg intensity. Magnetic susceptibility data in the inset of panel (a) show the SC transition.

correspondence to the symmetry of the observed signal.²⁷ The wave vector $\mathbf{Q} = (HKL)$ is given in reciprocal-lattice units (r.l.u.), i.e., in units of the reciprocal-lattice vectors of the Fe sublattice, in which the AFM ordering vector is $\mathbf{Q}_{\text{AFM}} = (\frac{1}{2} 0 \frac{1}{2})$. These measurements were done with a fixed final neutron momentum, $k_f = 2.662 \text{ \AA}^{-1}$, and with a pyrolytic graphite filter to eliminate higher-order reflections from the analyzer. In the paramagnetic state (Fig. 2, circles), a commensurate peak is observed at the ordering vector down to the lowest energies, indicating the presence of gapless paramagnon excitations. Below the AFM ordering temperature, its intensity vanishes in the low-energy region, below the spin gap energy [panels (a) and (c)], or gets partially suppressed at intermediate energies close to the gap onset [panel (b)]. For BaFe_2As_2 , we also show the corresponding scan centered at $L = 2$ [at the magnetic zone boundary, panel (d)], where the situation is similar with the exception of a reduced intensity of the signal. The presence of a relatively strong paramagnetic intensity on the $(\frac{1}{2} 0 L)$ line even far away

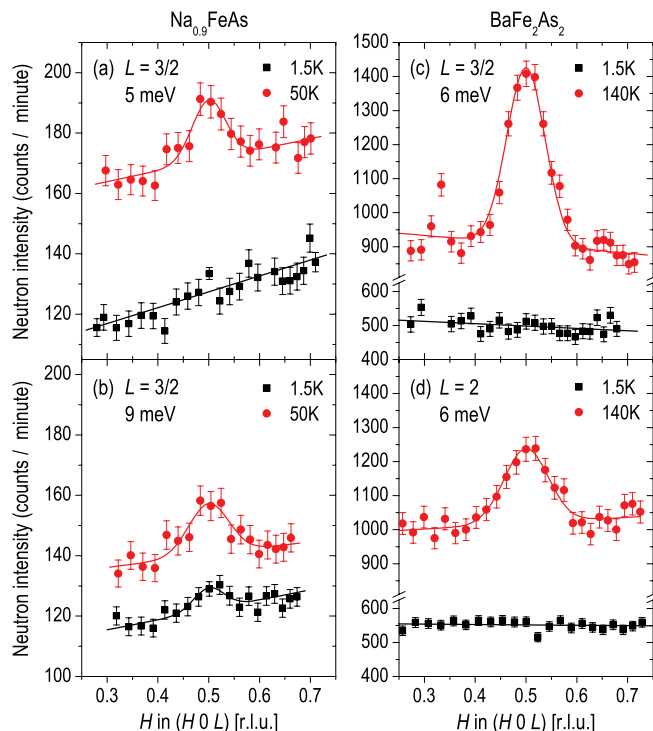


FIG. 2. (Color online) Typical unprocessed constant-energy scans for $\text{Na}_{0.9}\text{FeAs}$ (left) and BaFe_2As_2 (right), measured above and below T_N along the $|\mathbf{Q}| = \text{const}$ trajectories in momentum space, centered at $(\frac{1}{2}0L)$. The values of L at the center of the scan and the energy transfer are indicated in every panel.

from the ordering wave vector has been already pointed out in earlier works.^{10,11} It can be well understood in terms of Fermi surface nesting, which is maximized near \mathbf{Q}_{AFM} , but still remains substantial for all values of L , according to band structure calculations.²⁷

B. Temperature dependence

The detailed temperature dependence of the low-energy INS signals in both samples is illustrated by Fig. 3. Again, one can appreciate the similarity between the magnetic response measured at \mathbf{Q}_{AFM} (half-integer L) and at the magnetic zone boundary (integer L) in BaFe_2As_2 at an energy transfer of 6 meV [Fig. 3(b)]. Despite the somewhat lower amplitude of the signal at $(\frac{1}{2}02)$ as compared to $(\frac{1}{2}0\frac{3}{2})$, both increase monotonically upon cooling towards T_N , where they exhibit a sharp kink due to the onset of the spin gap in the AFM ordered state. This anomaly is much sharper at \mathbf{Q}_{AFM} due to the critical scattering intensity at the ordering wave vector around T_N .

It is remarkable that despite the presence of two well-separated phase transitions in $\text{Na}_{1-\delta}\text{FeAs}$, the low-energy magnetic spectrum is only sensitive to the AFM transition and exhibits no pronounced anomaly at T_s outside of our experimental uncertainty [Fig. 3(a)]. It is interesting to consider this observation in the framework of various models describing the electronic “nematic” state that was claimed responsible for the orthorhombic distortion in the narrow temperature range $T_N < T < T_s$.²⁸ Since a comprehensive theory of such a “nematic” electronic state in iron arsenides

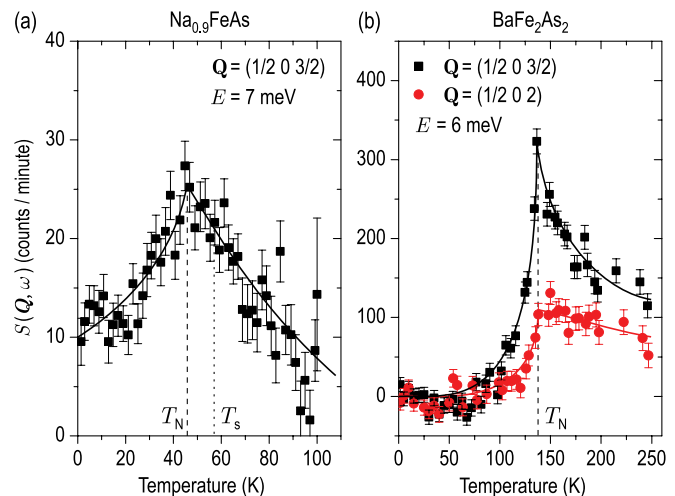


FIG. 3. (Color online) Temperature dependence of the background-subtracted low-energy INS signal in $\text{Na}_{0.9}\text{FeAs}$ (left) and BaFe_2As_2 (right), indicating the abrupt spin-gap opening below T_N . Solid lines are guides to the eyes. Note the absence of any pronounced anomaly at the structural phase transition in $\text{Na}_{0.9}\text{FeAs}$ ($T_s = 57$ K).

still awaits development, no definitive predictions about its magnetic excitation spectrum have been proposed. It has been recently suggested, however, that with the onset of a preemptive nematic order, the magnetic correlation length should discontinuously increase below T_s , leading to a possible spectral weight redistribution and a consequent formation of a pseudogap.²⁹ This could possibly result in a partial precursor gapping of the low-energy spin excitations already below T_s , which is not confirmed by our measurements.

C. Spin-gap magnitudes in $\text{Na}_{0.9}\text{FeAs}$ and BaFe_2As_2

In Fig. 4, we plot the energy dependence of the background-subtracted magnetic intensity, obtained from Gaussian fits of the momentum scans similar to those shown in Fig. 2 (larger symbols) or from 3-point measurements, in which the background intensity was obtained at two points on both sides of the peak (smaller symbols). Measurements with $k_f = 2.662 \text{ \AA}^{-1}$, $k_f = 3.837 \text{ \AA}^{-1}$, and $k_f = 4.1 \text{ \AA}^{-1}$ are shown with different symbols. In the paramagnetic state, a gapless spectrum of spin fluctuations with nearly energy-independent intensity is observed both at integer and half-integer L . As the temperature is decreased below the AFM transition, the low-energy spectral weight is transferred to higher energies, resulting in a clear spin gap in the magnetic excitation spectrum (see also Fig. 3). At \mathbf{Q}_{AFM} (half-integer L), the onset of magnetic intensity at $T = 1.5$ K is observed at approximately ~ 10 meV both in the $\text{Na}_{0.9}\text{FeAs}$ and BaFe_2As_2 compounds, so that the low-temperature spectra in Figs. 4(a) and 4(b) are nearly indistinguishable within the experimental uncertainty. Based on the recent polarized INS measurements,¹² we can ascribe this onset to the smaller out-of-plane anisotropy gap. The onset of the in-plane scattering that occurs at a slightly higher energy cannot be resolved as a separate step in our unpolarized data.

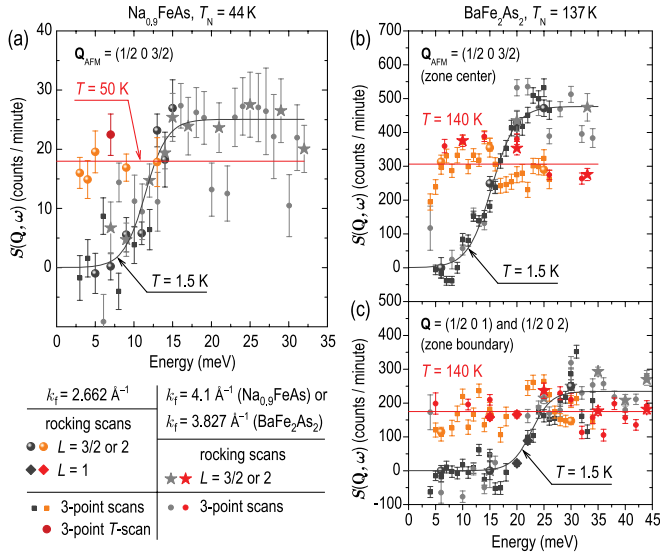


FIG. 4. (Color online) Energy dependence of the background-subtracted magnetic INS intensity for $\text{Na}_{0.9}\text{FeAs}$ (left) and BaFe_2As_2 (right), measured above and below T_N : (a), (b) at the ordering wave vector ($L = 3/2$) and (c) at the magnetic zone boundary ($L = 1, 2$).

At the magnetic zone boundary (integer L), the gap in BaFe_2As_2 is only twice larger than at the zone center and amounts to approximately 20 meV, in agreement with the assumptions of Ref. 30. This clearly refutes the commonly accepted viewpoint that zone-boundary spin waves in BaFe_2As_2 are limited to high energies of the order of 50–100 meV.^{6,12} In terms of the Heisenberg-type exchange interaction constants, our result suggests a much weaker out-of-plane exchange coupling, J_c , than previously estimated from fitting high-energy TOF data to the anisotropic Heisenberg model.⁶ Indeed, assuming the in-plane exchange interactions (J_{1a} , J_{1b} , and J_2) of Ref. 6 to be unchanged, we can use the zone-center and zone-boundary gap magnitudes from our present study (10 and 20 meV, respectively) to re-estimate the two remaining parameters in the model: the effective out-of-plane exchange energy, $SJ_c = 0.22$ meV, and the single-ion anisotropy constant, $SJ_s = 0.14$ meV. This reevaluated value of J_c is almost one order of magnitude smaller than previously reported,⁶ leading to a better agreement with the spin-wave

velocities estimated from the nuclear-magnetic-resonance data.³¹

IV. SUMMARY AND DISCUSSION

In Table I, we have summarized several parameters of the AFM state, such as the Néel temperature (T_N), value of the ordered magnetic moment (μ_{Fe}), and zone-center gap energy (Δ_{QAFM}) for various iron-arsenide compounds. First, we observe that despite the tenfold difference in the ordered magnetic moment and a much lower ordering temperature, $\text{Na}_{0.9}\text{FeAs}$ exhibits an anisotropy gap of the same order of magnitude as the materials of the “122” family. This is highly unusual, as theory predicts the anisotropy gap in spin-density-wave compounds to increase monotonically with the value of the sublattice magnetization, following a simple power law,³⁵ whereas our observations point to an anomalous behavior of the magnetocrystalline anisotropy in iron pnictides that is inconsistent with this general trend.

Second, we note that in “122” compounds the spin gap is rapidly reduced upon doping Ni or Co into the Fe plane. As a result, in the doping range, where superconductivity coexists with static AFM order, spin fluctuations can already be observed below T_N at energies as low as 2–3 meV.^{30,36} Whenever these fluctuations extend below the energy of the SC gap, 2Δ , they can possibly serve as a source of spectral weight for the formation of a magnetic resonant mode below T_c , which has been reported even in strongly underdoped “122” samples with T_c as low as 11 K.³⁶ In contrast to this scenario, superconductivity in the phase diagram of doped NaFeAs is found in the immediate vicinity of the parent phase,^{20,21} where we have shown the anisotropy gap to be much larger than 2Δ . Indeed, for our sample with $T_c = 8$ K, even the exceptionally high ratio of $2\Delta/k_B T_c \approx 8$ reported by Liu *et al.*³⁷ would result in 2Δ of only 5.5 meV, whereas the weak-coupling ratio of $2\Delta/k_B T_c = 3.53$ yields $2\Delta = 2.4$ meV, which is 4 times smaller than the magnetic anisotropy gap. Therefore, if the conventional scenario for the formation of the magnetic resonant mode also holds in the Na-111 family of superconductors, only 1–2% of Co or Ni would have to induce a substantial rearrangement of the low-energy magnetic spectral weight in NaFeAs , in order to reduce the zone-center gap and lead to a finite magnetic intensity below 2Δ . Further INS experiments on doped samples are required to explore the

TABLE I. Comparison of the Néel temperatures (T_N), values of the ordered magnetic moment (μ_{Fe}), and zone-center gap energies (Δ_{QAFM}) in several iron-arsenide compounds.

Compound	T_N (K)	μ_{Fe}/μ_B	Δ_{QAFM} (meV)	Ref.
SrFe_2As_2	205	1.0 (Ref. 32)	6.5	8
CaFe_2As_2	172	0.8 (Ref. 33)	6.9(2)	9,10
BaFe_2As_2	137	0.9 (Refs. 22,34)	7.7(2)	7
			9.8(4)	11
			10.1 (out-of-plane)	12
			16.4 (in-plane)	12
			10(1)	our work
$\text{Na}_{1-\delta}\text{FeAs}$	45	0.1 (Refs. 19,21)	10(2)	our work
$\text{BaFe}_{1.96}\text{Ni}_{0.04}\text{As}_2$	91		~ 2	30

interplay between magnetism and superconductivity in this system.

ACKNOWLEDGMENTS

The authors are grateful to G. Khaliullin, A. Yaresko, N. Shannon, and A. Smerald for fruitful discussions and thank J. White and C. Busch for the assistance in sample characterization. All presented INS data were collected using the triple-axis thermal-neutron spectrometer IN8 at the Institut

Laue-Langevin (ILL) in Grenoble. This work has been supported, in part, by the DFG within the Schwerpunktprogramm 1458, under Grant No. BO3537/1-1, and by the MPI-UBC Center for Quantum Materials. B.H.M. and Y.S.K. acknowledge support from the Basic Science Research Program (Grant No. 2010-0007487) and the Mid-career Researcher Program (Grant No. 2010-0007487) through NRF funded by the Ministry of Education, Science, and Technology of Korea. Y.L. acknowledges support from the Alexander von Humboldt Foundation.

*yskwon@dgist.ac.kr

†d.inosov@fkf.mpg.de

¹Y. Kamihara, H. Hiramatsu, M. Hirano, R. Kawamura, H. Yanagi, T. Kamiya, and H. Hosono, *J. Am. Chem. Soc.* **128**, 10012 (2006); Y. Kamihara, T. Watanabe, M. Hirano, and H. Hosono, *ibid.* **130**, 3296 (2008); C. Wang, L. Li, S. Chi, Z. Zhu, Z. Ren, Y. Li, Y. Wang, X. Lin, Y. Luo, S. Jiang, X. Xu, G. Cao, and Z. Xu, *EPL* **83**, 67006 (2008); G. Wu, Y. L. Xie, H. Chen, M. Zhong, R. H. Liu, B. C. Shi, Q. J. Li, X. F. Wang, T. Wu, Y. J. Yan, J. J. Ying, and X. H. Chen, *J. Phys.: Condens. Matter* **21**, 142203 (2009); M. Rotter, M. Tegel, and D. Johrendt, *Phys. Rev. Lett.* **101**, 107006 (2008); D. R. Parker, M. J. Pitcher, P. J. Baker, I. Franke, T. Lancaster, S. J. Blundell, and S. J. Clarke, *Chem. Commun.* 2189 (2009).

²For reviews, see G. R. Stewart, *Rev. Mod. Phys.* **83**, 1589 (2011); D. C. Johnston, *Adv. Phys.* **59**, 803 (2010); M. D. Lumsden and A. D. Christianson, *J. Phys.: Condens. Matter* **22**, 203203 (2010); C. W. Chu, *Nat. Phys.* **5**, 787 (2009).

³J. Paglione and R. L. Greene, *Nat. Phys.* **6**, 645 (2010).

⁴J. Zhao, D. T. Adroja, D.-X. Yao, R. Bewley, S. Li, X. F. Wang, G. Wu, X. H. Chen, J. Hu, and P. Dai, *Nat. Phys.* **5**, 555 (2009).

⁵S. O. Diallo, V. P. Antropov, T. G. Perring, C. Broholm, J. J. Pulikkotil, N. Ni, S. L. Bud'ko, P. C. Canfield, A. Kreyssig, A. I. Goldman, and R. J. McQueeney, *Phys. Rev. Lett.* **102**, 187206 (2009).

⁶L. W. Harriger, H. Q. Luo, M. S. Liu, C. Frost, J. P. Hu, M. R. Norman, and P. Dai, *Phys. Rev. B* **84**, 054544 (2011).

⁷R. A. Ewings, T. G. Perring, R. I. Bewley, T. Guidi, M. J. Pitcher, D. R. Parker, S. J. Clarke, and A. T. Boothroyd, *Phys. Rev. B* **78**, 220501(R) (2008).

⁸J. Zhao, D.-X. Yao, S. Li, T. Hong, Y. Chen, S. Chang, W. Ratcliff, J. W. Lynn, H. A. Mook, G. F. Chen, J. L. Luo, N. L. Wang, E. W. Carlson, J. Hu, and P. Dai, *Phys. Rev. Lett.* **101**, 167203 (2008).

⁹R. J. McQueeney, S. O. Diallo, V. P. Antropov, G. D. Samolyuk, C. Broholm, N. Ni, S. Nandi, M. Yethiraj, J. L. Zarestky, J. J. Pulikkotil, A. Kreyssig, M. D. Lumsden, B. N. Harmon, P. C. Canfield, and A. I. Goldman, *Phys. Rev. Lett.* **101**, 227205 (2008).

¹⁰S. O. Diallo, D. K. Pratt, R. M. Fernandes, W. Tian, J. L. Zarestky, M. Lumsden, T. G. Perring, C. L. Broholm, N. Ni, S. L. Bud'ko, P. C. Canfield, H.-F. Li, D. Vaknin, A. Kreyssig, A. I. Goldman, and R. J. McQueeney, *Phys. Rev. B* **81**, 214407 (2010).

¹¹K. Matan, R. Morinaga, K. Iida, and T. J. Sato, *Phys. Rev. B* **79**, 054526 (2009).

¹²N. Qureshi, P. Steffens, S. Wurmehl, S. Aswartham, B. Buchner, and M. Braden, *arXiv:1201.2332*.

¹³A. N. Yaresko, G.-Q. Liu, V. N. Antonov, and O. K. Andersen, *Phys. Rev. B* **79**, 144421 (2009).

¹⁴K. Sasmal, B. Lv, Z. J. Tang, F. Chen, Y. Y. Xue, B. Lorenz, A. M. Gulov, and C. W. Chu, *Phys. Rev. B* **79**, 184516 (2009).

¹⁵Y. J. Song, J. S. Ghim, B. H. Min, Y. S. Kwon, M. H. Jung, and J.-S. Rhyee, *Appl. Phys. Lett.* **96**, 212508 (2010).

¹⁶I. Todorov, D. Y. Chung, H. Claus, C. D. Malliakas, A. P. Douvalis, T. Bakas, J. He, V. P. Dravid, and M. G. Kanatzidis, *Chem. Mater.* **22**, 3916 (2010).

¹⁷Y. Liu, D. L. Sun, J. T. Park, and C. T. Lin, *Physica C* **470**, S513 (2010); D. L. Sun, J. Z. Xiao, and C. T. Lin, *J. Cryst. Growth* **321**, 55 (2011).

¹⁸G. F. Chen, W. Z. Hu, J. L. Luo, and N. L. Wang, *Phys. Rev. Lett.* **102**, 227004 (2009).

¹⁹S. Li, C. de la Cruz, Q. Huang, G. F. Chen, T.-L. Xia, J. L. Luo, N. L. Wang, and P. Dai, *Phys. Rev. B* **80**, 020504(R) (2009).

²⁰D. R. Parker, M. J. P. Smith, T. Lancaster, A. J. Steele, I. Franke, P. J. Baker, F. L. Pratt, M. J. Pitcher, S. J. Blundell, and S. J. Clarke, *Phys. Rev. Lett.* **104**, 057007 (2010).

²¹J. D. Wright, T. Lancaster, I. Franke, A. J. Steele, J. S. Moller, M. J. Pitcher, A. J. Corkett, D. R. Parker, D. G. Free, F. L. Pratt, P. J. Baker, S. J. Clarke, and S. J. Blundell, *Phys. Rev. B* **85**, 054503 (2012).

²²Q. Huang, Y. Qiu, W. Bao, M. A. Green, J. W. Lynn, Y. C. Gasparovic, T. Wu, G. Wu, and X. H. Chen, *Phys. Rev. Lett.* **101**, 257003 (2008).

²³S. Nandi, M. G. Kim, A. Kreyssig, R. M. Fernandes, D. K. Pratt, A. Thaler, N. Ni, S. L. Bud'ko, P. C. Canfield, J. Schmalian, R. J. McQueeney, and A. I. Goldman, *Phys. Rev. Lett.* **104**, 057006 (2010).

²⁴C. Lester, J.-H. Chu, J. G. Analytis, S. C. Capelli, A. S. Erickson, C. L. Condon, M. F. Toney, I. R. Fisher, and S. M. Hayden, *Phys. Rev. B* **79**, 144523 (2009).

²⁵D. K. Pratt, W. Tian, A. Kreyssig, J. L. Zarestky, S. Nandi, N. Ni, S. L. Bud'ko, P. C. Canfield, A. I. Goldman, and R. J. McQueeney, *Phys. Rev. Lett.* **103**, 087001 (2009).

²⁶A. Kreyssig, M. G. Kim, S. Nandi, D. K. Pratt, W. Tian, J. L. Zarestky, N. Ni, A. Thaler, S. L. Bud'ko, P. C. Canfield, R. J. McQueeney, and A. I. Goldman, *Phys. Rev. B* **81**, 134512 (2010); K. Marty, A. D. Christianson, C. H. Wang, M. Matsuda, H. Cao, L. H. Van Bebber, J. L. Zarestky, D. J. Singh, A. S. Sefat, and M. D. Lumsden, *ibid.* **83**, 060509(R) (2011); K. Prokeš, S. Mat'áš, L. Harnagea, S. Singh, S. Wurmehl, D. N. Argyriou, and B. Büchner, *ibid.* **83**, 104414 (2011).

²⁷J. T. Park, D. S. Inosov, A. Yaresko, S. Graser, D. L. Sun, Ph. Bourges, Y. Sidis, Y. Li, J.-H. Kim, D. Haug, A. Ivanov, K. Hradil, A. Schneidewind, P. Link, E. Faulhaber, I. Glavatskyy, C. T. Lin, B. Keimer, and V. Hinkov, *Phys. Rev. B* **82**, 134503 (2010).

- ²⁸C. Fang, H. Yao, W.-F. Tsai, J. P. Hu, and S. A. Kivelson, *Phys. Rev. B* **77**, 224509 (2008); I. I. Mazin and M. D. Johannes, *Nat. Phys.* **5**, 141 (2009).
- ²⁹R. M. Fernandes, A. V. Chubukov, J. Knolle, I. Eremin, and J. Schmalian, *Phys. Rev. B* **85**, 024534 (2012).
- ³⁰L. W. Harriger, A. Schneidewind, S. Li, J. Zhao, Z. Li, W. Lu, X. Dong, F. Zhou, Z. Zhao, J. Hu, and P. Dai, *Phys. Rev. Lett.* **103**, 087005 (2009).
- ³¹K. Kitagawa, N. Katayama, K. Ohgushi, M. Yoshida, and M. Takigawa, *J. Phys. Soc. Jpn.* **77**, 114709 (2008); A. Smerald and N. Shannon, *Phys. Rev. B* **84**, 184437 (2011).
- ³²K. Kaneko, A. Hoser, N. Caroca-Canales, A. Jesche, C. Krellner, O. Stockert, and C. Geibel, *Phys. Rev. B* **78**, 212502 (2008); J. Zhao, W. Ratcliff, J. W. Lynn, G. F. Chen, J. L. Luo, N. L. Wang, J. Hu, and P. Dai, *ibid.* **78**, 140504(R) (2008); Y. Lee, D. Vaknin, H. Li, W. Tian, J. L. Zarestky, N. Ni, S. L. Bud'ko, P. C. Canfield, R. J. McQueeney, and B. N. Harmon, *ibid.* **81**, 060406(R) (2010).
- ³³A. I. Goldman, D. N. Argyriou, B. Ouladdiaf, T. Chatterji, A. Kreyssig, S. Nandi, N. Ni, S. L. Bud'ko, P. C. Canfield, and R. J. McQueeney, *Phys. Rev. B* **78**, 100506(R) (2008).
- ³⁴S. D. Wilson, Z. Yamani, C. R. Rotundu, B. Freelon, E. Bourret-Courchesne, and R. J. Birgeneau, *Phys. Rev. B* **79**, 184519 (2009).
- ³⁵R. S. Fishman and S. H. Liu, *Phys. Rev. B* **58**, R5912 (1998); **59**, 8681 (1999).
- ³⁶A. D. Christianson, M. D. Lumsden, S. E. Nagler, G. J. MacDougall, M. A. McGuire, A. S. Sefat, R. Jin, B. C. Sales, and D. Mandrus, *Phys. Rev. Lett.* **103**, 087002 (2009).
- ³⁷Z.-H. Liu, P. Richard, K. Nakayama, G.-F. Chen, S. Dong, J.-B. He, D.-M. Wang, T.-L. Xia, K. Umezawa, T. Kawahara, S. Souma, T. Sato, T. Takahashi, T. Qian, Y. Huang, N. Xu, Y. Shi, H. Ding, and S.-C. Wang, *Phys. Rev. B* **84**, 064519 (2011).